

The existence of a special surface film or skin layer on the surface of water was discovered at the beginning of the present century. The important role of this film in natural hydrophysical processes was subsequently revealed [1, 2]. The surface film on water is a dynamic structure — it forms convergence zones and surface eddies; because of its reduced temperature it continuously forms convection currents, which penetrate into the water. The investigation of the structure of the surface film and its interaction with the deep layers of water requires the application of very diverse techniques. In the last decade investigations by laboratory modeling have been the most intensive [3, 4].

In this paper we give the results of laboratory investigations of surface microconvection with the aid of fluorescent dyes in conjunction with the shadow method. The fluorescent-dye method is convenient because it is highly sensitive to hydrodynamic processes and it requires the addition of the tracer in such low concentration that the indicator impurity almost completely satisfied the condition of inertness and stability; at the same time, it allows the differentiation of individual elementary volumes of liquid in a complicated hydrodynamic movement.

Experimental Method. The experiments were conducted in rectangular cells ( $150 \times 150 \times 500 \text{ mm}^3$ ) with transparent glass walls. For the experiments we used distilled and doubly distilled water. To exclude the direct effect of the atmosphere and to reduce the vertical momentum we covered the water surface with a 3-5-mm layer of dodecane — a high-molecular-weight liquid paraffin which is insoluble in water and does not dissolve water. As fluorescent dyes we used fluorescein, rhodamine B, eosin, etc. We detected no differences in their behavior during the experiments and, hence, in this paper we give the results obtained with fluorescein. The fluorescence was excited by the light of a mercury lamp through an illuminator fitted with a heat-absorbing cell and a set of interchangeable filters. The processes were recorded by photography.

Results and Discussion. As the experiments showed, a drop of dye solution introduced into the dodecane layer passed through the water surface and formed an annular eddy, which penetrated into the water, and broke up in cascade fashion into numerous secondary annular eddies. This process depended on the size of the drop and the concentration of the indicator dye. The optimal drop size for eddy formation was approximately  $0.1\text{--}0.2 \text{ cm}^3$ . If the dye concentration in the drop was less than  $10^{-6}$  mole/liter a single annular eddy was usually formed; when the concentration was  $10^{-5}\text{--}10^{-2}$  mole/liter the cascade breakup of the initial eddy was clearly expressed.

If the dye concentration was more than  $10^{-2}$  mole/liter the dye solution spread rapidly over the water surface due to the change in surface tension and formed a molecular film. The dye concentration on the surface when the drop spread out was reduced by 4-5 orders, the effect of the dye on the properties of the water become insignificant, and the skin layer was formed again on the water surface. On the elapse of 30-35 sec (the relaxation time of the dye-stained surface film) convection currents flowed from the water surface into the water. A photograph of the development of this process is shown in Fig. 1a.

We observed two forms of free convection currents from the water surface. The usual form was a jet with a spherical lower tip and was apparently a weakly developed eddy. In addition, convection currents in the form of vertical films were formed from the convergence bands in the surface film. On the leading edge of these films weak eddies of droplike shape were also formed. Sometimes we observed detachment of the frontal eddies from the convection jet.

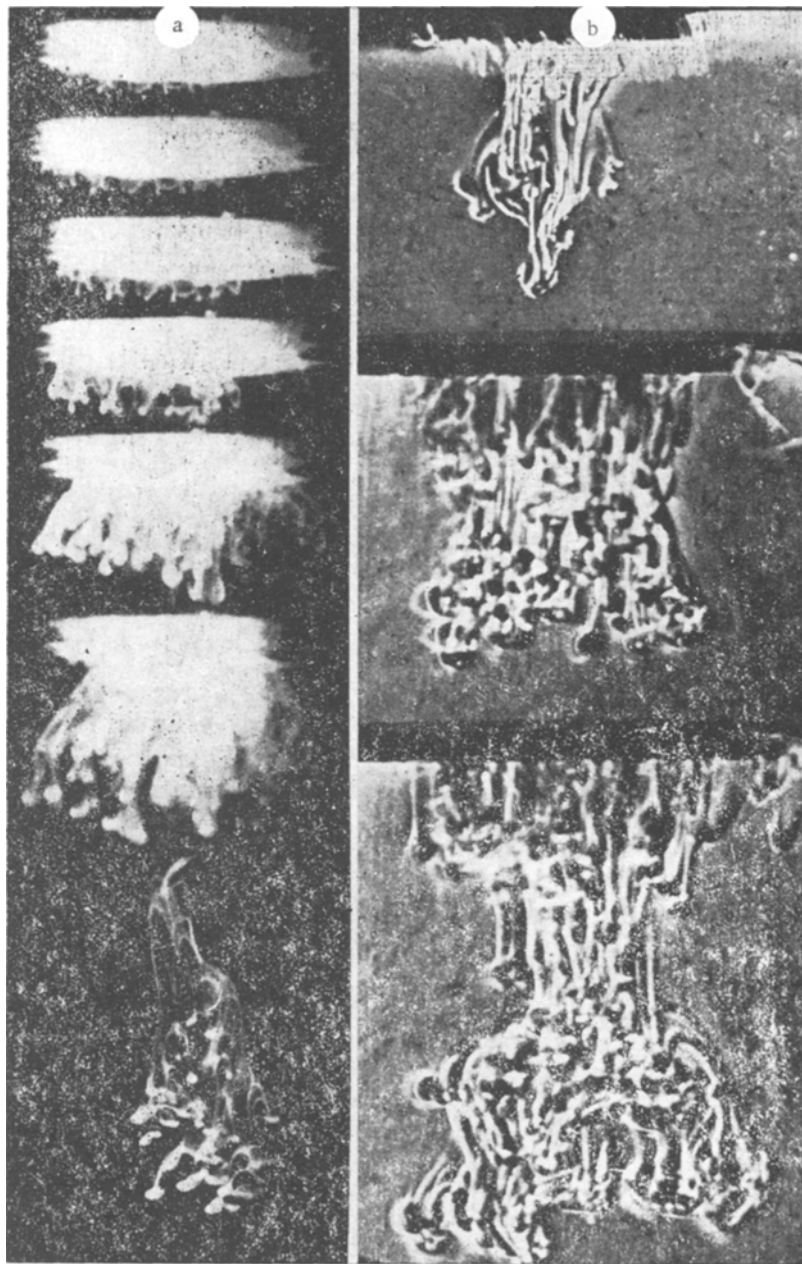


Fig. 1

Comparative visualization of the picture of convection currents from the surface by the shadow method, without the use of dyes (Fig. 1b), and by the fluorescence method described here, showed that they were identical. This indicates that the dissolved indicator dye did not cause any distortions in the investigated system and at the same time made it possible to distinguish individual microconvection currents.

Kinetic curves of the descent of the convection currents, measured from the position of their fronts on the obtained photographs, are shown in Fig. 2, where curve 1 is the kinetic curve calculated from the averaged results of synchronous measurement of the descent of six convection jets. The limits of the spread shown on the curve do not indicate the error of measurement, but the difference in the behavior of individual convection jets. The pronounced differences can be attributed to the oscillations associated with the descent, which disturb the monotonic course of the flow. These oscillations could be detected by photographing the movement of a single drop as it passed through the surface and formed an annular eddy. The kinetic curves of the oscillatory motion are shown by lines 3 in Fig. 2, for which the depths  $z$  are indicated in brackets on the left of the  $y$  axis (3-1 corresponds to the movement of the leading eddy, 3-3 corresponds to the increase in its horizontal

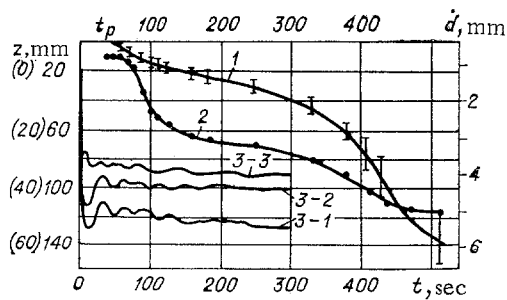


Fig. 2

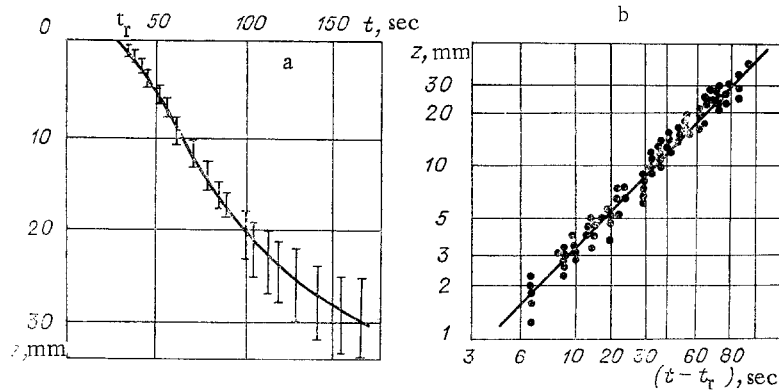


Fig. 3

TABLE 1

| Depth z, mm | Speed of descent, $u = \frac{\partial z}{\partial t}$ , cm/sec | $Re = \frac{\rho u d}{\mu}$ | $Fr = \frac{u^2}{gd}$  |
|-------------|--|-----------------------------|------------------------|
| <1          | $<3 \cdot 10^{-3}$   | $\leq 3 \cdot 10^{-2}$      | $<9 \cdot 10^{-8}$     |
| 1-17        | $3 \cdot 10^{-3}$  | $(3-7) \cdot 10^{-2}$       | $(9-4) \cdot 10^{-8}$  |
| 15-45       | $1,8 \cdot 10^{-3}$  | $(4-6) \cdot 10^{-2}$       | $1 \cdot 10^{-8}$      |
| 50-110      | $1 \cdot 10^{-2}$  | $4 \cdot 10^{-1}$           | $2 \cdot 10^{-7}$      |
| >100        | $<3 \cdot 10^{-3}$   | $>10^{-1}$                  | $\sim 2 \cdot 10^{-8}$ |

diameter, 3-2 corresponds to the height of the wake remaining in the form of a jet). An interesting feature was the spatial synchronization of the oscillatory motion of a convection jet of complex shape. Curve 2, Fig. 2, shows the averaged increase in diameter of the leading eddies of convection jets corresponding to the kinetic curve 1. The depths  $z$  for curve 2 are indicated on the right on the y axis.

An analysis of the kinetics of the near-surface convective motion revealed irregular behavior with time as the liquid descended into the deeper layers, and several regions with appreciably different speeds could be distinguished. The dynamic characteristics of these distinct regions, calculated from the kinetic curves, are given in Table 1 with a correction for the relaxation time of the surface film  $t_r = 30-35$  sec.

The initial region of convective flow to a depth  $z = 30$  mm, which took place in approximately 160 sec, was satisfactorily approximated by a power function of the parabolic type  $z = 0.25 (t - t_r)^{1.05}$  mm. This relation is shown in Fig. 3. If the relaxation time is ignored, microconvection in this surface layer is approximated by the relation  $z = 294 t^{0.059} - 365$  mm.

The low values of the Reynolds and Froude numbers, given in Table 1, where  $d$  is the diameter of the droplet tip of the convection jet, and the other symbols are generally known, show that the main factors in the development of microconvection are generally viscosity  $\mu u/d^2$ , and that inertial forces  $\rho u^2/d$  are of less importance. With increase in the depth of propagation of microconvection  $d$  increases (curves 2, 3, Fig. 2), which together with the change in speed of penetration leads to some increase in  $Re$ .

The reasons for the discovered variation in speed of the convection currents will require further investigations. For instance, the initial portion to a depth  $z = 20$  mm is probably associated with the motion of the leading, weakly developed eddies. This hypothesis is consistent with increase in their diameters on the time curve (curve 2, Fig. 2).

We know from studies of the skin layer on a water surface that the hydrophysical properties of near-surface water layers, beginning at the first millimeter layer, are different [3-6]. A fluorescent dye, as a tracer distributed at the molecular level, is probably sensitive to such fine changes in hydrophysical properties.

A possible reason for the observed changes is the stratification of the near-surface water layers, produced by microconvection of the upper, colder, water film. As our experiments indicated, as distinct from immiscible liquids, where the stable form of existence is a spherical drop, the passage of a drop through the surface of a homogeneous liquid, particularly water, converts it to an annular or toroidal eddy, due to which this element of the liquid receives an initial momentum, as curves 3, Fig. 2, show. The energy source of this process is obviously the energy of surface tension of the liquid.

On reaching a certain depth (see Fig. 2), the penetrating liquid element is subject to oscillatory movements due to buoyancy forces. The period of such oscillations is  $T \cong 35$  sec. This period obviously corresponds to the buoyancy frequency (the Brandt-Weizel frequency)  $N(z) = 2\pi/T = 6.28/35 \cong 0.2 \text{ sec}^{-1}$  when  $\rho = 0.999 \text{ g}\cdot\text{cm}^{-3}$  (density of water at  $19^\circ\text{C}$ ) and  $g = 981 \text{ cm}\cdot\text{sec}^{-2}$  (gravitational acceleration). From this we can determine the density gradient formed in the water due to microconvection of the surface film:  $-\partial\rho/\partial z = N(z)^2\rho/g \cong 4\cdot 10^{-5} \text{ g}\cdot\text{cm}^{-2}$ . This value is in good agreement with the results of determination of the density gradient by interferometric measurements [4].

It follows from this that such a gradient at depth  $\sim 3$  cm (curves 3, Fig. 2) is due to the difference in water density relative to the surface  $\Delta\rho \cong \Delta z 4\cdot 10^{-5} = 1.2\cdot 10^{-4} \text{ g}\cdot\text{cm}^{-3}$ . Knowing this difference we can determine the difference between the surface film temperature and the water layer at depth 3 cm from the equation of state of water; the difference is  $0.6\text{--}0.7^\circ\text{C}$ . This value, calculated from fluorimetric measurements, is in good agreement with the temperature difference obtained in laboratory and field conditions by direct experimental measurements [2-6].

On the basis of the obtained results we note the following.

Molecular layers of a fluorescent dye applied to a water surface constitute a sensitive probe for the detection of hydrophysical near-surface processes.

Water drops passing through the surface film into the water form annular or toroidal eddies in the absence of vertical momentum.

The speed of microconvection currents from the water surface is variable and is  $\sim 10^{-3} \text{ cm}\cdot\text{sec}^{-1}$  on the average for  $Re = 10^{-2}\text{--}10^{-1}$  and  $Fr = 10^{-7}\text{--}10^{-8}$ .

The penetration of microconvection currents to a depth of  $z = 3$  cm is approximated by a power function  $z = 0.25(t - t_r)^{1.05} \text{ mm}$ , where  $t_r = 30\text{--}35$  sec. If the relaxation time is ignored this approximation has the form  $z = 294 t^{0.059} - 365 \text{ mm}$ .

Microconvection currents stratify the near-surface water layers so that the experimentally measured buoyancy frequency at depth  $z = 3$  cm is  $0.2 \text{ sec}^{-1}$ , which corresponds to a density gradient  $\sim 4\cdot 10^{-5} \text{ g}\cdot\text{cm}^{-2}$  and a temperature difference relative to the surface of  $0.6\text{--}0.7^\circ\text{C}$ .

#### LITERATURE CITED

1. N. N. Zubov, "A remarkable case of ice formation," *Meteorol. Vestn.*, Nos. 10-12 (1934).
2. R. D. Hudson, *Infrared System Engineering*, Wiley, New York (1969).
3. *Convective Mixing in the Sea* [in Russian], Moscow State Univ., Moscow (1977).
4. A. I. Ginzburg and K. N. Fedorov, "Contribution of salinity and temperature to the development of convection during evaporation of sea water," in: *Study of the Variability of Physical Processes in the Ocean* [in Russian], Inst. Okeanologii Akad. Nauk SSSR, Moscow (1978).
5. E. D. McAllister and W. McLeish, "Heat transfer in the top millimeter of the ocean," *J. Geophys. Res.*, 74, No. 13 (1969).

6. R. S. Bortkovskii, É. K. Byutner, S. P. Malevskii-Malevich, and L. Yu. Preobrazhenskii, *Transport Processes near the Ocean-Atmosphere Interface [in Russian]*, Gidrometeoizdat, Leningrad (1974).

THEORY OF INTERACTION OF GRAVITY WAVES WITH HYDRODYNAMIC  
TURBULENCE

A. G. Sazontov

UDC 532.517.4+532.59

1. One of the practical problems in atmospheric and ocean dynamics is the study of the effect of vortex turbulence on the propagation of various types of waves (surface waves, sound, internal waves, etc.). Besides, it is necessary to differentiate the strictly hydrodynamic turbulence from vortex motions accompanying waves [1, 2]. The numerous aspects of the interaction of sound with turbulence have been analyzed in fairly great detail so far (see [3-5] and the literature cited in them). The study of the vortex-wave turbulence with reference to the interaction of gravity waves with vortices is continued in this paper. It is worth emphasizing that unlike [3-5], the present problem has a number of special features associated with the fact that surface waves in deep water are dispersive, the phase velocity  $v_\phi$  is a function of wavelength  $\lambda$ :  $v_\phi = \sqrt{g\lambda}$  ( $g$  is the acceleration of gravity,  $\lambda = \lambda/2\pi$ ). The logarithmic decrement for gravity waves propagating at the surface of a turbulent liquid has been found on the basis of computed matrix of interaction coefficients. An estimate of the characteristic phase correlation time and the time for making the wave field isotropic in elastic scattering have been obtained. The diffusion approximation has been used to analyze the effect of inelastic scattering on the development of isotropic wave packets as a function of frequency. The limits of the applicability of kinetic equations to describe the mutual interaction of gravity waves in a turbulent medium have been explained. All these problems have been analyzed within the framework of a single formal scheme, viz., the Wyld diagram technique [6].

2. Consider the motion of an incompressible fluid with a free surface of infinite depth. We choose a coordinate system with the  $z$  axis vertically up. Let the surface shape be given by the function  $z = \eta(r_\perp, t)$  with the normal  $\mathbf{n} = [1 + (\nabla_\perp \eta)^2]^{-1/2} \times (-\nabla_\perp \eta, 1)$ .

The kinematic boundary condition

$$\partial \eta / \partial t + (\mathbf{u} \nabla_\perp) \eta = u_z \quad (2.1)$$

is satisfied at the free surface. It couples  $\eta$  to the fluid velocity  $\mathbf{u}$ , which is governed by the equations

$$\partial \mathbf{u} / \partial t + (\mathbf{u} \nabla) \mathbf{u} = -(1/\rho) \nabla p + \mathbf{g}; \quad (2.2)$$

$$\operatorname{div} \mathbf{u} = 0. \quad (2.3)$$

Here  $p$  is the pressure,  $\rho$  is the density,  $\mathbf{g}$  is the acceleration of gravity. The system of equations (2.1)-(2.3) is completed by the dynamic boundary condition at the free surface\*

$$p|_{z=\eta} = 0 \quad (2.4)$$

(in which a constant atmospheric pressure is taken as the reference value) and the condition of boundedness of fields as  $z \rightarrow -\infty$ .

In such a system there are, in general, two types of motions: vortex motion (hydrodynamic turbulence) and potential motion (surface waves). Hence it is convenient to divide the velocity field into two parts:

$$\mathbf{u} = \mathbf{u}^l + \mathbf{u}^t, \operatorname{rot} \mathbf{u}^l = 0, \operatorname{div} \mathbf{u}^t = 0, \quad (2.5)$$

\*Surface tension has been neglected here and in what follows.